Antarctic Bottom Water Sensitivity to Spatio-Temporal Variations in Antarctic Meltwater Fluxes

Wilton Aguiar[1,2,3] , **Sang-Ki Lee**[2] , **Hosmay Lopez**[2] , **Shenfu Dong**[2] , **Hélène Seroussi**[4] , **Dani C. Jones**[5] , and **Adele K. Morrison**[3]

[1]Cooperative Institute for Marine and Atmospheric Studies, University of Miami, Miami, FL, USA, [2]NOAA, Atlantic Oceanographic and Meteorological Laboratory, Miami, FL, USA, [3]Research School of Earth Sciences, Australian Centre for Excellence in Antarctic Science, The Australian National University, Acton, ACT, Australia, [4]Thayer School of Engineering, Dartmouth College, Hanover, NH, USA, [5]British Antarctic Survey, Natural Environment Research Council, UK Research and Innovation, Cambridge, UK

Abstract Ice sheet melting into the Southern Ocean can change the formation and properties of the Antarctic Bottom Water (AABW). Ocean models often mimic ice sheet melting by adding freshwater fluxes in the Southern Ocean under diverse spatial distributions. We use a global ocean and sea-ice model to explore whether the spatial distribution and magnitude of meltwater fluxes can alter AABW properties and formation. We find that a realistic spatially varying meltwater flux sustains AABW with higher salinities compared to simulations with uniform meltwater fluxes. Finally, we show that increases in ice sheet melting above 12% since 1958 can trigger AABW freshening rates similar to those observed in the Southern Ocean since 1990, suggesting that the increasing Antarctic meltwater discharge can drive the observed AABW freshening.

Plain Language Summary Previous research suggests that increased Antarctic ice sheet (AIS) melting may be driving freshening in the abyssal Southern Ocean, and Antarctic sea ice expansion since 1978. However, the main tools we have to assess abyssal ocean changes are ocean models, and they often misrepresent Antarctic ice melting by assuming it occurs uniformly along the Antarctic coast. In this study, we use a global ocean model to assess if correcting the spatial distribution of Antarctic ice melting (from uniform to spatially varying), and increasing its magnitude, can change the salinity in the abyssal Southern Ocean. We show that correcting the spatial representation of the AIS melting results in abyssal waters with higher salinities, correcting 30% the ocean model fresh bias in the abyssal cells. We also show that a 12% increase in Antarctic ice melting can trigger freshening of the abyssal Southern Ocean at rates similar to the trends observed since the 1990s, thus suggesting that enhanced melting of Antarctic land ice may be the main driver of the recently observed AABW freshening.

1. Introduction

AABW formation is one of the main components of the Global Meridional Overturning Circulation (GMOC), a large-scale ocean circulation system that connects all ocean basins and controls global climate stability (Talley, 2013). Freshwater originating from the Antarctic ice sheet (AIS) enters the ice shelf cavities and marginal seas, lowering local salinities and potentially hindering the formation of Antarctic Bottom Water (AABW) (Silvano et al., 2018; Wijk & Rintoul, 2014). Thus, by changing the rate of AABW formation, AIS melting can significantly affect the state of the global climate.

AABW is mainly formed at the Antarctic margins through interaction between the ocean, sea ice and ice shelves. Along the ice shelves, brine rejection and buoyancy loss in coastal polynyas forms the dense shelf water (DSW), a precursor water for AABW. DSW then flows through the continental shelf, forming AABW through further mixing with circumpolar deep water (CDW) along the continental shelf break (Carmack & Foster, 1975; Foster & Carmack, 1976). Ice melting also occurs under ice shelves, releasing freshwater and thus decreasing salinities along the Antarctic coast. Hence, increasing AIS melting can increase the buoyancy of DSW, hindering the formation of AABW (Wijk & Rintoul, 2014). Alternatively, AABW can be formed offshore by deep convection in open-ocean polynyas (e.g., Killworth, 1983), a process commonly present in models (Aguiar et al., 2017; Azaneu et al., 2013), but only observed a few times since satellites started monitoring sea ice in the Southern Ocean in late 1972 (Campbell et al., 2019; Gordon, 1978).

Methodology: Wilton Aguiar, Sang-Ki Lee, Hosmay Lopez, Shenfu Dong, Hélène Seroussi, Dani C. Jones, Adele K. Morrison
Project Administration: Sang-Ki Lee, Hosmay Lopez, Shenfu Dong
Resources: Hosmay Lopez
Software: Dani C. Jones
Supervision: Wilton Aguiar, Sang-Ki Lee, Hosmay Lopez, Shenfu Dong, Adele K. Morrison
Validation: Wilton Aguiar, Sang-Ki Lee, Hosmay Lopez, Shenfu Dong, Dani C. Jones, Adele K. Morrison
Visualization: Wilton Aguiar, Adele K. Morrison
Writing – original draft: Wilton Aguiar
Writing – review & editing: Wilton Aguiar, Sang-Ki Lee, Hosmay Lopez, Shenfu Dong, Hélène Seroussi, Dani C. Jones, Adele K. Morrison

Two main processes release meltwater from AIS to the Southern Ocean. First, while circulating within ice-shelf cavities, warm CDW exchanges heat with the overlying ice and induces melting on the ice shelf base, a process known as *basal melting* (Jenkins et al., 2001). Second, ice can detach from the ice shelves creating icebergs - a process referred to as *calving* (e.g., Joughin & MacAyeal, 2005). Detached icebergs are advected by surface winds and ocean currents (e.g., Wagner et al., 2017), releasing freshwater along their advective path. Besides their potential impact on AABW formation, increased ocean surface stratification driven by ice shelf basal melting and calving are thought to increase sea-ice coverage (Bintanja et al., 2013). However, most climate and ocean models do not have interactive ice-shelves, making it difficult to understand the impact of ice sheet melting on AABW formation and sea ice area (Jongma et al., 2009).

Coupling ice sheet models to ocean and sea-ice models to simulate AIS melting is technically complex and requires considerable computational effort (Nowicki & Seroussi, 2018). An alternative approach is to add freshwater fluxes in the Southern Ocean. Climate models often estimate the AIS melting from the difference of precipitation minus evaporation over Antarctica (P-E) routed to the coast through the Antarctic drainage basin. This approach yields a valid estimate for the total AIS melting when the AIS is assumed to be under equilibrium surface mass balance. However, the spatial distribution of runoff fluxes derived from P-E over Antarctica will greatly differ across climate models, while AIS melting is mostly concentrated along the west Antarctica (Depoorter et al., 2013). For example, basal mass loss in the Amundsen Sea is estimated to be about 484 Gt yr^{-1}, six times higher than in the Ross Sea shelf (79 Gt yr^{-1}, based on surface mass balance for the Antarctic Ice Shelf from 2009 to 2012) (Depoorter et al., 2013). The representation of ice runoff from P-E freshwater fluxes could impose salinity biases under ice shelf cavities, changing the salinity of AABW and its source waters (Jongma et al., 2009). Therefore, it is important to assess how the spatial distribution of AIS melting impacts AABW properties. Furthermore, a significant freshening of the AABW over the last three decades has been reported (Anilkumar et al., 2021; Purkey & Johnson, 2012), with regional increases in AIS melting and calving possibly triggering this freshening (Fogwill et al., 2015). This connection between enhanced regional AIS melting and AABW freshening makes it even more critical to assess how spatial variations in AIS melting alter AABW properties.

Therefore, this work assesses the impact of the freshwater distribution on AABW properties and transport in a global ocean and sea-ice model and further analyzes the potential response of AABW to an enhanced AIS melting.

2. Methods

2.1. CESM1

All simulations were performed using the ocean and sea-ice components of the Community Earth System Model version 1 (CESM1) (Danabasoglu et al., 2012) from the National Center for Atmospheric Research. The ocean component of CESM1 is the Parallel Ocean Program version 2, while sea ice is simulated by the Community Ice Code version 4 (CICE) (Danabasoglu et al., 2012). Ocean and sea ice were forced with surface fluxes from the European Center for Medium-Range Weather Forecast ERA5 reanalysis for the 1958–1980 period (Hersbach et al., 2020). A horizontal resolution of ∼1° was used for both ocean and sea-ice components. We chose to use the 1° low-resolution version of the CESM1 instead of an eddy-rich resolution (<10 km) so the simulations can be integrated over a long period of one thousand years to assure equilibrium in the deep branch of the overturning circulation. The ocean is divided into 60 unevenly-spaced levels, with thicknesses ranging from 10 m at the surface to 250 m in the deep ocean. All simulations were initialized with temperature and salinity fields from the Polar Hydrographic Climatology (Steele et al., 2001). A spin-up approach from Lee et al. (2017, 2019) is followed here where each year in the model is forced with randomly chosen historic fields from ERA5.

Most of the widely used ocean and sea ice models inaccurately represent AABW formation. A possible reason for this misrepresentation is that most models' current horizontal and vertical resolutions are too coarse to reproduce the downslope flow of dense waters off the Antarctic shelf and its mixing along the way, an essential process to form AABW (Mensah et al., 2021). Coarse resolution models exhibit excessive mixing of DSWs as they flow over the shelf break and down the slope, decreasing the density and inhibiting AABW formation from shelf-sourced dense waters (Heuzé et al., 2013). Instead, these models create AABW through deep convection in the open ocean, resulting in bottom waters that are often too fresh (Heuzé, 2021). An overflow parameterization
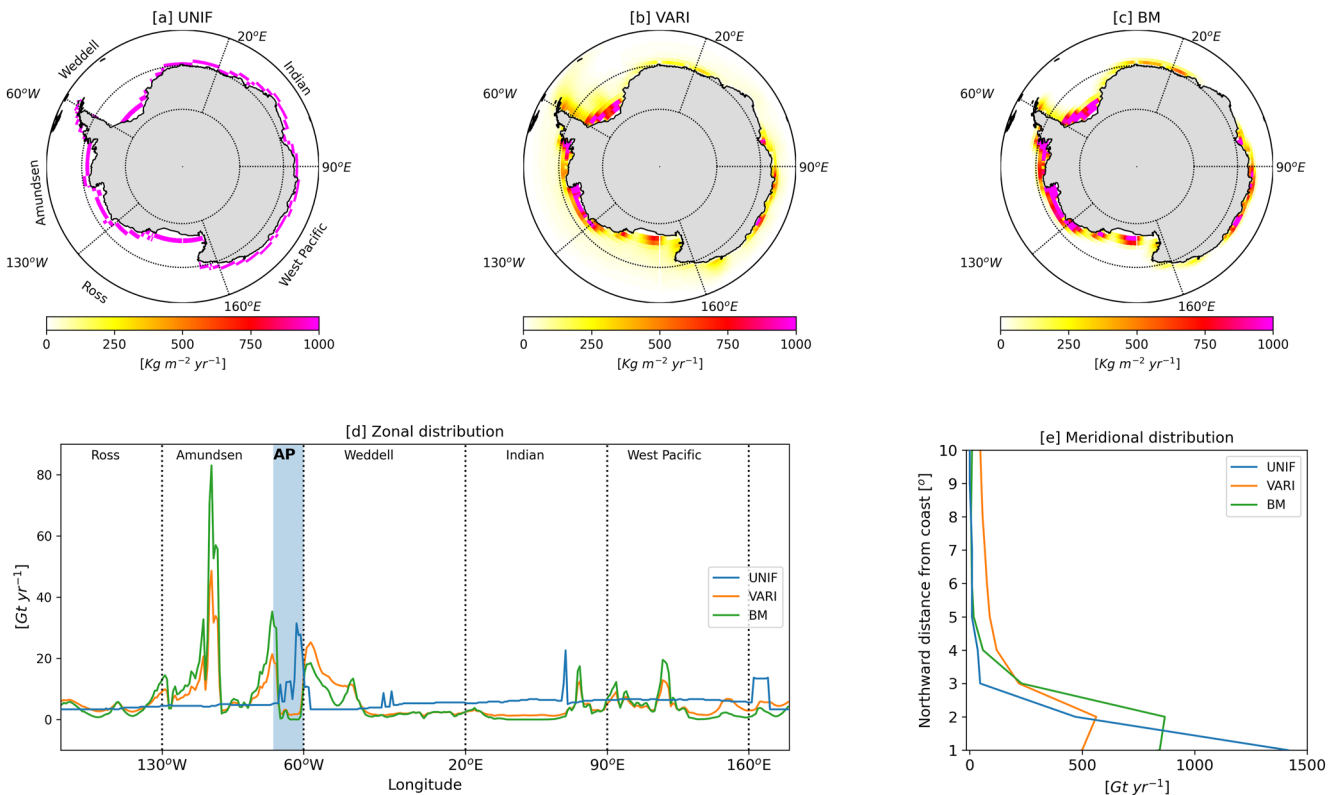
Figure 1. Freshwater flux fields used to force the model simulations (a–c). Southern Ocean sectoral division is shown in (a). Plotted in (d) are the zonal distributions of freshwater fluxes that are integrated meridionally. The blue band marks the location of the Antarctic Peninsula. Plotted in (e) is the meridional distribution of the zonally integrated freshwater fluxes, as a function of the meridional distance from the Antarctic Coast.

is employed in CESM1 to better represent the downslope flow of AABW (Danabasoglu et al., 2012). It has been shown that the overflow parameterization significantly improves AABW formation in CESM2 (Heuzé, 2021), which shares the same ocean and sea ice components with CESM1. Therefore CESM1 was used in this study.

2.2. Water Masses

We define AABW as the waters with a neutral density higher than 28.27 kg m^{-3} (Orsi & Wiederwohl, 2009). AABW salinity was calculated as the average salinity of AABW waters south of 60°S. The Southern Ocean was divided into five sectors (Figure 1a) according to Parkinson and Cavalieri (2012): the Weddell Sector, Indian Sector, West Pacific, Ross Sector, and Amundsen Sector. The AABW transport in the Southern Ocean was measured as the absolute value of the minimum of the streamfunction at 65°S in density coordinates. The confidence interval for the AABW transport was obtained from the 95% confidence level of the yearly-averaged AABW transport estimates from the last 100 years of each simulation. Finally, although basal melting occurs under both ice shelves and icebergs, in this study the term basal melting specifically refers to melting under ice shelves.

2.3. Freshwater Distribution Simulations

We carried out three model simulations to test to what extent AABW formation and salinity are affected by the spatio-temporal distribution of Antarctic meltwater fluxes. Since the AIS runoff can differ between climate models, in the first experiment we chose to use a uniformly distributed freshwater flux, which is the simplest AIS melting distribution we can use as reference. The first experiment (*UNIF*, as in uniform) was forced with a freshwater flux of 2075 Gt/yr added uniformly in the ocean grid points closest to the Antarctic coast (Figure 1a; Table S1 in Supporting Information S1). The flux magnitude of 2075 Gt/yr is based on total ice mass loss estimates from Rignot et al. (2019), and a full derivation of the value can be found in Text S2 in Supporting Information S1. The freshwater flux field of *UNIF* does not account for the spatial variation in freshwater fluxes from calving or basal melting.

The second simulation (*BM*) was forced with zonally varying fluxes to mimic the horizontal variations in AIS basal melting (Figure 1c). The third simulation (*VARI*, Figure 1b) was forced with a freshwater flux that mimics the spatial variation of both ice shelf basal melting and calving (Text S1 in Supporting Information S1). The spatial distribution of basal melting takes into account the meltwater production of Antarctic ice shelves estimated by Rignot et al. (2013), while iceberg melting distribution is based on satellite-tracked iceberg positions from 1979 until 2017 (Text S2 in Supporting Information S1). *VARI* differs from *BM* in the meridional distribution of freshwater fluxes, that is, by having part of its freshwater fluxes displaced offshore, as seen by the higher melting fluxes offshore (Figure 1d, northward distances from coast larger than 3° of latitude), and lower melting fluxes along the coast (Figure 1d, distances lower than 3°) in *VARI* compared to *BM*. The spatially varying freshwater flux fields used in *VARI* and *BM* simulations were produced according to the method discussed in Hammond and Jones (2016). All freshwater fluxes were applied at the surface of the ocean model. Although ice shelf basal melting may occur down to 1 km in the water column, freshwater fluxes from basal melting are often added to the ocean surface by the modeling community (e.g., CORE2), as in (Farneti et al., 2015; Griffies et al., 2009). Therefore, we applied this approach for simplicity, and to assure applicability to other ocean models. Although the spatial distribution of freshwater fluxes in *BM*, *VARI*, and *UNIF* differs, the total freshwater flux is the same in all simulations. Additionally, we analyzed what we define here as the overflow salinity error, that is, the terrain-following salinity error along the southern most limit of the domain, from the continental shelf until the abyssal plains. This overflow salinity error is calculated for the deepest cells at each longitude and latitude, using as a reference the World Ocean Atlas 2018 climatology for the period between 1955 and 1974, interpolated onto the CESM1 grid.

2.4. Increased Ice Melting Experiment

Recent observational studies showed that AIS melting increased up to 40% from 1994 to 2018 (Adusumilli et al., 2020; Rignot et al., 2019). It has been suggested that this enhanced AIS melting rate is responsible for the observed AABW freshening in the last three decades (e.g., Anilkumar et al., 2021). To test if the enhanced AIS melting can explain the observed freshening trend in AABW (Menezes et al., 2017; Shimada et al., 2012), we performed three additional simulations with increases in the AIS freshwater flux according to observed historical ice discharge estimates (Rignot et al., 2019). Starting from the initial conditions, the simulation *R12* is forced with the total ice discharge fluxes from 1978 until 2017 obtained from Rignot et al. (2019), with fluxes linearly extended back to the 1958 value of 2075 Gt/yr. This simulation amounts to a 12% increase in AIS melting over 60 years (Figure S3 in Supporting Information S1). Two additional scenarios of increased ice sheet melting were designed based on the maximum ice discharge from Rignot et al. (2019) for 2017 and its standard deviation. First, a minimum increase scenario with a 5% increase in melting (*R05*), and second a maximum increase scenario with an 18% increase in melting (*R18*). Simulations *R05*, *R12,* and *R18* were branched from year 901 of *VARI*. The only transience in the *R* simulations is due to the historically increasing AIS melting fluxes. The years 901–1000 of the equilibrium simulation (*VARI*) were used to determine the natural variability of salinity in the model. *VARI* was linearly detrended to avoid models drifts to alter the measured natural variability. The same trend was removed from the *R* experiments for consistency. Finally, *R5*, *R12* and *R18* all share the non-uniform freshwater flux distribution from *VARI*.

For comparison with previous observations of AABW freshening, the bottom layer freshening in those experiments was calculated in two ways. First, the increase in the freshwater column below 4,000 m depth and south of 60°S was converted in $cm\ yr^{-1}$ unit to compare it with spatial observations from Purkey and Johnson (2012). Second, regionally mean profiles of salinity change were calculated for the Australian-Antarctic basin (AAB, between 80°E and 150°E), Weddell-Enderby basin (WEB, between 60°W and 80°E), and the Amundsen-Bellingshausen basin (ABB, between 150°E and 60°W, Figure 3b). The computed basin-averaged freshening rates were compared to observations by Jullion et al. (2013), Menezes et al. (2017), Purkey and Johnson (2012), Purkey et al. (2019), and Shimada et al. (2012).

3. Results

3.1. Uniform Versus Spatially Varying Freshwater Fluxes

Compared to the uniform freshwater flux experiment (*UNIF*), results from the spatially varying freshwater flux experiment (*VARI,* Figure 2) show significant salinity anomalies. At the surface, the Amundsen Sea coast
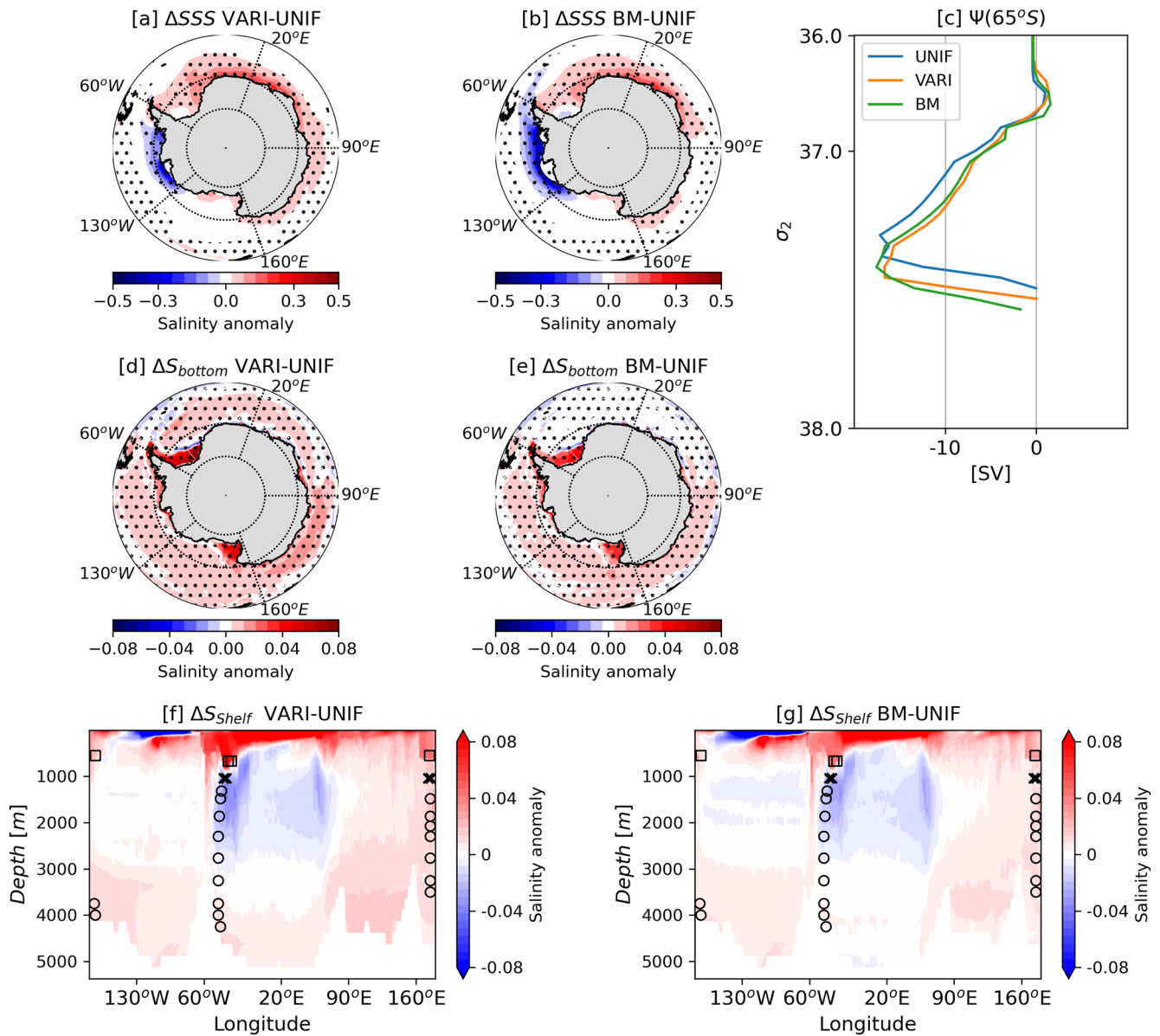
Figure 2. Effects of meltwater redistribution. (a, b) are anomalies in sea surface salinity (ΔSSS), (d, e) are bottom ocean salinity anomalies (ΔS_{bottom}), (c) is the ocean overturning in density space at 65°S, and (f, g) are salinity anomalies on the ocean cells closest to the Antarctic coast (ΔS_{shelf}). (a, d) are salinity anomalies for *VARI-UNIF*, and (b, e) are anomalies for *BM-UNIF*. Dotted areas indicate regions of statistically significant anomalies at a 95% confidence level from a student *t*-test. On panels (f) and (g) squares mark the source water locations, circles show entrainment locations and ×'s show the exit water locations for the shelf overflow parameterization (Text S3 in Supporting Information S1).

becomes 0.5 ± 0.12 fresher in *VARI* while the remaining Antarctic coast increases in salinity by up to 0.2 ± 0.07 (Figure 2a), thus reflecting the concentration of the freshwater fluxes along the Amundsen Sea (Figure 1d). In the bottom layer, salinity in the Southern Ocean (i.e., poleward of 60°S) increases up to 0.1 ± 0.06 (Figure 2d) in *VARI*. The average AABW salinity increases by $1.9 \pm 0.60 \times 10^{-3}$ in *VARI* compared to *UNIF*. Thus, the bottom cell of the Southern Ocean's overturning circulation extends to denser waters, but the transport of the bottom cell stays approximately the same between the *UNIF* and *VARI* (Figure 2c).

We constructed a transect along the southernmost limit of the domain to see how shelf salinity anomalies propagate through the overflow path (Figure 2f). This terrain-following plot shows that positive surface salinity anomalies in the *VARI* experiment are advected downwards along the shelf to the bottom layer (Figure 2f). The downward advection of high salinity anomalies happens mostly where the shelf overflow is parameterized in
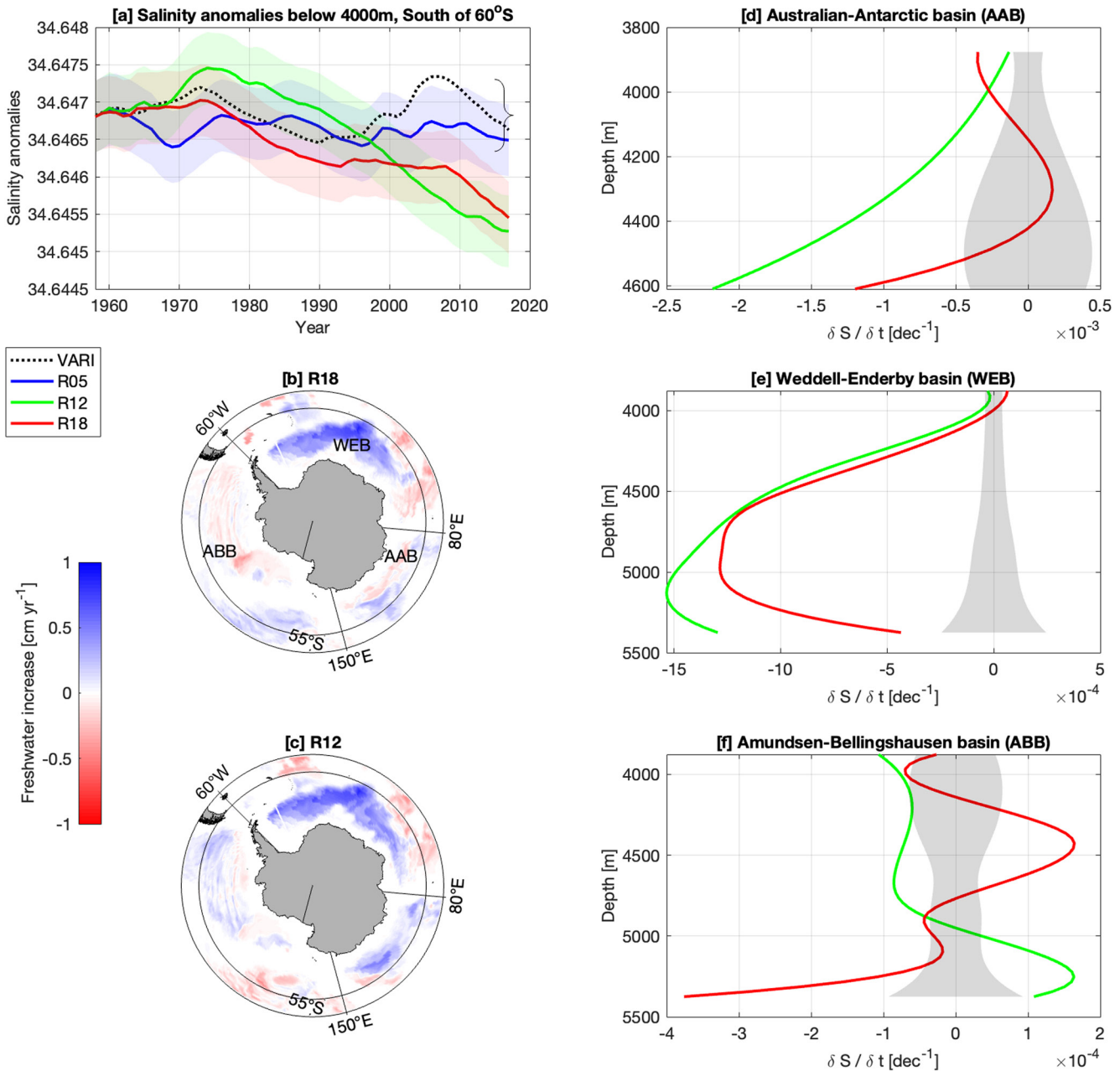
Figure 3. Effects of increased Antarctic ice sheet melting. In (a) are plotted time series of mean ocean salinity anomaly below 4,000 m depth and South of 60°S for the scenarios *R05* (blue), *R12* (green), *R18* (red), and for the equilibrium simulation *VARI* (black). The curly bracket corresponds to the amplitude of the salinity natural variability in VARI of 4.8×10^{-3}, and the shading shows are the AABW salinity anomaly in each simulation $\pm 4.8 \times 10^{-3}$. (b, c) show the rate of change in freshwater content below 4,000 m depth for the experiments *R18* and *R12*. Southern Ocean basins are separated by the 60°W, 80°E, 150°E meridians, and correspond to the Weddell-Enderby basin, Australian-Antarctic basin, and Amundsen-Bellingshausen basin. (d–f) are the average rate of salinity change in each basin as a function of depth. Gray shadows represent the minimum rate of salinity change required to surpass the signal of natural variability.

CESM1 (circles in Figure 2f). Therefore, the overflow parameterization has a key role in transmitting surface salinity signals to the deep ocean. Once in the bottom layer, the positive salinity anomalies spread laterally increasing the AABW salinity across the Southern Ocean (Figure 2f).

Finally, adding a spatially varying freshwater flux at the surface (Figures 2d and 2f) has an important role in correcting the AABW salinity biases in CESM1. Under the uniform surface freshwater forcing, the overflow salinity error (see Section 2.4) is up to -0.034 (Figure S6 in Supporting Information S1, $z = 4,100$ m). This error

is reduced to −0.024 under the spatially varying freshwater flux (Figure S6 in Supporting Information S1), which is a 30% reduction in salinity error at the continental margins of the Southern Ocean.

There are a few possible reasons why the spatially varying freshwater flux in *VARI* increases surface salinity over most of the Antarctic coast. First, *VARI* has lower freshwater fluxes over most of the Antarctic coast except in the Amundsen Sea compared to *UNIF* (Figure 1d). These lower freshwater fluxes may increase surface salinities along most of the Antarctic coast compared to UNIF-except in the Amundsen Sea where larger freshwater fluxes may decrease the surface waters' salinity (Figures 2a and 2f). Second, surface freshwater fluxes in *VARI* are also redistributed meridionally to represent both ice shelf basal melting and icebergs melting away from the coast (Figures 1b and 1e). In other words, a portion of the freshwater flux applied along the coast in *UNIF* was redistributed offshore in *VARI* (Figure 1e). This meridional redistribution can further reduce the freshwater fluxes over most of the Antarctic coast, resulting in higher salinities in *VARI*.

To test to what extent zonally varying freshwater fluxes cause the salinity changes in the surface and bottom layer of *VARI*, we compare *UNIF* with *BM* which represents the zonally varying ice shelf basal melting without iceberg melting (Figure 1c). Zonal variations in freshwater fluxes in *BM* reproduce the same surface and bottom layer signals seen in *VARI*. In particular, *BM* shows higher surface salinities along most of the Antarctic shelf except in the Amundsen Sea (Figure 2b). This surface signal is carried into bottom waters (Figure 2e) through shelf overflow (Figure 2g). The Southern Ocean overturning in *BM* also maintains its strength, similar to the *VARI* case (Figure 2c). Therefore, zonally varying freshwater fluxes (Figures 1c and 1d, *BM*) result in the same increase in AABW and surface salinities as in the case of the zonally and meridionally varying meltwater fluxes (as in *VARI*). Further evaluation of the effects of iceberg melting versus ice shelf basal melting confirms that the meridional displacement of freshwater fluxes has minimal effect on AABW transport and salinity (Text S5 in Supporting Information S1). This result suggests that zonal variation in freshwater input along the Antarctic coast is primarily responsible for increasing AABW salinity and surface salinity along the Weddell and the Ross Sea sectors in the *VARI* simulation, while the meridional variation has a relatively small impact, mostly in the open Weddell Sea and the Indian Ocean sectors (Figure 2d).

3.2. AABW Response to Increased AIS Melting

To investigate the transient response to an increase in AIS melting fluxes, we evaluated how AABW responds to three historical scenarios of increased ice sheet melting. In the *R12* and *R18* scenarios, increased AIS melting resulted in decreasing of the AABW salinity from 1974 until 2017 at a magnitude higher than the natural variability threshold (Figure 3a). For the low freshwater increase scenario (*R05*) all the AABW salinity anomaly is contained within the natural variability of the model, and therefore they cannot be attributed to changes in the surface freshwater fluxes. The mean AABW freshening in the *R12* and *R18* scenarios are 0.5×10^{-3} dec^{-1} and 0.4×10^{-3} dec^{-1} respectively. Zonal means of salinity anomalies for *R12* and *R18* show waters with negative anomalies at the source and exit depths of the shelf overflow parameterization (Figure S4 in Supporting Information S1). This consistent bottom and shelf waters freshening under increased AIS melting suggests that the negative salinity anomalies on the Antarctic shelf in the *R12* and *R18* experiments are propagated to the bottom layer by the shelf overflow parameterizations. *R18* exhibits a weaker freshening rate of bottom waters compared to *R12*, even though the surface freshwater flux in *R18* is larger than in *R12*. However, the salinity timeseries of *R12* and *R18* overlap when considering the natural variability range (Figure 3a). Therefore, the difference in freshening rates between *R12* and *R18* is likely due to the natural variability of AABW salinity.

The increase in freshwater content below 4,000 m depth is only present in the WEB and the AAB-Figures 3b and 3c. For these sectors, the increase in the freshwater content is up to 1 cm yr^{-1} since 1978 for either simulation. This rate is similar to the freshwater column trends observed by Purkey and Johnson (2012) for the WEB (up to 1 cm yr^{-1}) and AAB (up to 1.5 cm yr^{-1}).

Regarding local salinity change, the maximum freshening happens around 4,600 m deep in AAB, at a rate of 2.2×10^{-3} dec^{-1} for *R12* and 1.3×10^{-3} dec^{-1} for *R18*. Based on observations in the AAB, Menezes et al. (2017) found a mean freshening of $2 \pm 1 \times 10^{-3}$ dec^{-1} (from 1994 to 2001), Shimada et al. (2012) found a mean AABW freshening rate of $2.7 \pm 0.4 \times 10^{-3}$ dec^{-1} (from 1990 to 2000). Purkey and Johnson (2012) found AABW (defined in their study as waters colder than 0°C) freshening ranging between 0.5×10^{-3} dec^{-1} and 4.1×10^{-3} dec^{-1} using several transects with the earliest observations in 1991 and latest in 2007. Therefore, the simulated and observed AABW freshening trends are similar in the AAB sector.

In the WEB, the maximum freshening for *R12* occurs at around 5,200 m (1.5×10^{-3} dec^{-1}), while for *R18* occurs around 4,900 m (1.3×10^{-3} dec^{-1}). These trends in the WEB are below the observed AABW freshening of $4 \pm 2 \times 10^{-3}$ dec^{-1} in the western Weddell Sea (from 1993 to 2011) obtained by Jullion et al. ([2013](#)). Purkey and Johnson ([2012](#)) observed a water mass freshening rates in WEB between 0.5×10^{-3} dec^{-1} and 1×10^{-3} dec^{-1}, that is, of the same magnitude as the ones simulated in *R12* and *R18*. On the other hand, Purkey and Johnson ([2012](#)) found that this water mass freshening was fully compensated by heaving isopycnals, causing no net salinity changes in mean AABW salinity. Nevertheless, for AAB and WEB, the increase in surface freshwater flux applied at CESM1 produced an AABW freshening at rates comparable to observations since 1990, suggesting that the observed freshening of AABW in these sectors could be driven by the historical increase in AIS melting.

In the ABB, no consistent salinity trend between simulations is found either spatially or in the spatial mean (Figures [3b](#), [3c](#), and [3f](#)). Purkey and Johnson ([2012](#)) did not find a statistically significant basin wide AABW freshening for the ABB either. In contrast, local AABW freshening trends at a transect just outside the Ross Sea suggest a strong freshening rate of 4×10^{-3} dec^{-1} (Purkey et al., [2019](#)). Possible reasons for this discrepancy are discussed in Section [4](#).

Finally, the sea ice area in the Southern Ocean expanded in *R12* from 1978 until 2005 at a rate of 2.4×10^3 km^3 yr^{-1} (Figure S5a in Supporting Information [S1](#)). This expansion is much smaller than the observed value of 33×10^3 km^3 yr^{-1} from 1979 to 2015 (Sun & Eisenman, [2021](#)). Furthermore, no sea ice expansion is present in *R05* or *R18* in the same period, suggesting that the small increase in the Southern Ocean sea ice area in *R12* does not arise from increased AIS melting. AABW transport at 65°S also exhibits no clear trend (Figure S5b in Supporting Information [S1](#)). The lack of consistent response of sea ice area and AABW transport to the increased freshwater flux suggests that the current increase in AIS melting is likely not large enough to cause substantial changes in the strength of the Southern Ocean overturning and sea ice production.

4. Discussion and Conclusions

Climate models often infer AIS meltwater fluxes through the difference between precipitation and evaporation on land, yielding spatial distributions of freshwater fluxes that do not match the observed AIS melting distribution (Rignot et al., [2013](#), [2019](#)). This spatial misrepresentation can create surface salinity biases that can propagate into AABW properties (Jongma et al., [2009](#)). In this study, five different freshwater flux experiments were carried out to better understand the AABW response to the location (uniform and varying) and to increasing AIS melting. Our results show that AABW salinity is sensitive to where the meltwater flows around the Antarctic continent (i.e., zonal distribution of freshwater fluxes). Varying the AIS melting fluxes zonally according to observations (*VARI*, Figures [1b](#) and [1d](#)) produces a $1.9 \pm 0.6 \times 10^{-3}$ increase in AABW salinity compared to a uniform meltwater flux. In *VARI*, the freshwater flux is the largest in the Amundsen sector (Figure [1d](#)) and smaller in the remaining regions along the Antarctic coast. As a result, surface salinity is increased across the Weddell and Ross Seas in *VARI* compared to *UNIF* (Figures [2a](#), [2d](#), and [2f](#)). The positive salinity anomalies in the Weddell and Ross Seas propagate to the bottom layer by the shelf overflow. The higher AABW salinity found in the experiment with spatially varying freshwater fluxes (*VARI*) has important implications for the representation of AABW in CESM1. Specifically, to reduce the AABW fresh bias in the CESM1 ocean component, arising from uniform AIS melting, a better practice is to force CESM1 with zonally varying fluxes that mimic the observed basal melting and calving distribution as in *VARI*. Although spatially varying, the P-E approximation of AIS melting in climate models do not account for the concentration of melting fluxes along the Amundsen and Bellingshausen seas (Figure [1d](#)). Therefore, spatially distributing this runoff according to AIS melting patterns (e.g., in *VARI*) can help reduce the fresh bias found in climate model's abyssal waters (Heuzé et al., [2013](#)). Further assessment should be done to identify if the same AABW fresh biases and correction can be applied in other ocean and sea ice models. This practice is also consistent with the surface meltwater flux protocol suggested in OMIP phase 2 (Tsujino et al., [2020](#)).

Finally, observations show that AABW salinity decreased since the 1980s (Menezes et al., [2017](#); Purkey & Johnson, [2012](#)). To investigate if AABW freshening in the Southern Ocean could be driven by increased AIS melting, we explored the sensitivity of AABW salinity to increases in meltwater fluxes of 5%, 12%, and 18% from 1958 until 2017, based on historical estimates of AIS melting from Rignot et al. ([2019](#)). For freshwater flux increase scenarios above 12%, AABW steadily freshens after 1978 in response to the increased freshwater flux.

The maximum AABW freshening rate simulated in this study occurs in the AAB (2.2×10^{-3} dec^{-1} and 1.3×10^{-3} dec^{-1} at 4,600 m in the ABB) and is consistent with freshening rates previously obtained by several observational studies (Menezes et al., 2017; Purkey & Johnson, 2012; Shimada et al., 2012). Increasing the freshwater fluxes by 12% or above triggered AABW freshening mostly in WEB and AAB basins, in agreement with observations reported by Purkey and Johnson (2012). The similarity of the AABW freshening rates simulated in the Australian-Antarctic and WEBs when forcing the ocean model with historically increased freshwater fluxes suggests that the observed AABW freshening in these sectors are likely triggered by the increase in AIS melting since 1990.

However, salinity trends in the abyssal ABB are inconsistent between the simulations (Figures 3b, 3c, and 3f). A possible reason for this discrepancy could be due to the advection route of the bottom waters formed along the Antarctic shelf. A high-resolution modeling study with accurate non-parameterized DSW formation shows that 98% of the bottom waters in ABB originate from DSW formed in the Ross Sea and Adelie Land (Solodoch et al., 2022), highlighting that lateral advection is essential for AABW to reach this basin. In CESM1, the shelf overflow parameterizations inject newly formed and fresher AABW on the slope directly below the formation site in the Weddell and Ross Sea shelves (Figures 2f and 2g). This direct vertical piping can hinder zonal advection of the newly formed AABW toward the deep ABB, therefore precluding this basin from exhibiting a consistent freshening signal.

In contrast with the simulated changes in AABW salinity, the AABW transport and the sea ice area in the Southern Ocean were insensitive to either the spatial distribution or to increases in AIS melting. Therefore, our simulations suggest that the historical increases in AIS melting cannot explain the sea ice expansion since 1980s nor imply that observed AABW freshening is accompanied by weaker AABW formation. This result should be taken with caution since AABW formation in the ocean component of CESM1 is conditioned by the shelf overflow parameterizations.

It is important to highlight that these results are constrained by the specific CESM1 configuration. For example, shelf overflow parameterizations play a critical role in propagating the surface salinity anomalies to the bottom layer in CESM1. Models with similar resolutions than CESM1 (~1°) often form AABW by open ocean deep convection, which can dampen the surface freshening by mixing the surface freshwater with high-salinity deep waters. Finally, ice shelves can reach down to 1 km in the water column and as such the freshwater fluxes from basal melting are not restricted to the surface as in our experiments. Ice shelf melting at deeper levels can induce coastal freshening rates different from those in our experiments (Pauling et al., 2016). Further studies are necessary to assess how specific model settings, such as eddy and shelf overflow parameterizations impact the AABW sensitivity to AIS melting.

Data Availability Statement

All the simulation's data used in this study are openly available at the Zenodo database, via https://doi.org/10.5281/zenodo.7416287, with unrestricted access conditions.

References

Adusumilli, S., Fricker, H. A., Medley, B., Padman, L., & Siegfried, M. R. (2020). Interannual variations in meltwater input to the Southern Ocean from Antarctic ice shelves. *Nature Geoscience*, *13*(9), 616–620. https://doi.org/10.1038/s41561-020-0616-zice

Aguiar, W., Mata, M. M., & Kerr, R. (2017). On deep convection events and Antarctic Bottom Water formation in ocean reanalysis products. *Ocean Science*, *13*(6), 851–872. https://doi.org/10.5194/os-13-851-2017

Anilkumar, N., Jena, B., George, J. V., Ravichandran, M., & S, K. (2021). Recent freshening, warming, and contraction of the Antarctic Bottom Water in the Indian sector of the Southern Ocean. *Frontiers in Marine Science*, *8*. https://doi.org/10.3389/fmars.2021.730630

Azaneu, M., Kerr, R., Mata, M. M., & Garcia, C. A. (2013). Trends in the deep Southern Ocean (1958–2010): Implications for Antarctic Bottom Water properties and volume export. *Journal of Geophysical Research: Oceans*, *118*(9), 4213–4227. https://doi.org/10.1002/jgrc.20303

Bintanja, R., van Oldenborgh, G. J., Drijfhout, S. S., Wouters, B., & Katsman, C. A. (2013). Important role for ocean warming and increased ice-shelf melt in Antarctic sea-ice expansion. *Nature Geoscience*, *6*(5), 376–379. https://doi.org/10.1038/ngeo1767

Campbell, E. C., Wilson, E. A., Moore, G. K., Riser, S. C., Brayton, C. E., Mazloff, M. R., & Talley, L. D. (2019). Antarctic offshore polynyas linked to Southern Hemisphere climate anomalies. *Nature*, *570*(7761), 319–325. https://doi.org/10.1038/s41586-019-1294-0

Carmack, E. C., & Foster, T. D. (1975). On the flow of water out of the Weddell Sea. *Deep Sea Research and Oceanographic Abstracts*, *22*(11), 711–724. https://doi.org/10.1016/0011-7471(75)90077-7

Danabasoglu, G., Bates, S. C., Briegleb, B. P., Jayne, S. R., Jochum, M., Large, W. G., & Yeager, S. G. (2012). The CCSM4 ocean component. *Journal of Climate*, *25*(5), 1361–1389. https://doi.org/10.1175/JCLI-D-11-00091.1

Depoorter, M. A., Bamber, J. L., Griggs, J. A., Lenaerts, J. T., Ligtenberg, S. R., van den Broeke, M. R., & Moholdt, G. (2013). Calving fluxes and basal melt rates of Antarctic ice shelves. *Nature*, *502*(7469), 89–92. https://doi.org/10.1038/nature12567

Farneti, R., Downes, S. M., Griffies, S. M., Marsland, S. J., Behrens, E., Bentsen, M., et al. (2015). An assessment of Antarctic Circumpolar Current and Southern Ocean meridional overturning circulation during 1958–2007 in a suite of interannual CORE-II simulations. *Ocean Modelling*, *93*, 84–120. https://doi.org/10.1016/j.ocemod.2015.07.009

Fogwill, C. J., Phipps, S. J., Turney, C. S. M., & Golledge, N. R. (2015). Sensitivity of the Southern Ocean to enhanced regional Antarctic ice sheet meltwater input. *Earth's Future*, *3*(10), 317–329. https://doi.org/10.1002/2015ef000306

Foster, T. D., & Carmack, E. C. (1976). Frontal zone mixing and Antarctic Bottom Water formation in the southern Weddell Sea. *Deep Sea Research and Oceanographic Abstracts*, *23*(4), 301–317. https://doi.org/10.1016/0011-7471(76)90872-X

Gordon, A. L. (1978). Deep Antarctic convection west of Maud Rise. *Journal of Physical Oceanography*, *8*(4), 600–612. https://doi.org/10.1175/1520-0485(1978)008<0600:DACWOM>2.0.CO;2

Griffies, S. M., Biastoch, A., Böning, C., Bryan, F., Danabasoglu, G., Chassignet, E. P., et al. (2009). Coordinated ocean-ice reference experiments (COREs). *Ocean Modelling*, *26*(1–2), 1–46. https://doi.org/10.1016/j.ocemod.2008.08.007

Hammond, M. D., & Jones, D. C. (2016). Freshwater flux from ice sheet melting and iceberg calving in the Southern Ocean. *Geoscience Data Journal*, *3*(2), 60–62. https://doi.org/10.1002/gdj3.43

Hersbach, H., Bell, B., Berrisford, P., Hirahara, S., Horányi, A., Muñoz-Sabater, J., et al. (2020). The ERA5 global reanalysis. *Quarterly Journal of the Royal Meteorological Society*, *146*(730), 1999–2049. https://doi.org/10.1002/qj.3803

Heuzé, C. (2021). Antarctic Bottom Water and North Atlantic deep water in CMIP6 models. *Ocean Science*, *17*(1), 59–90. https://doi.org/10.5194/os-17-59-2021

Heuzé, C., Heywood, K. J., Stevens, D. P., & Ridley, J. K. (2013). Southern Ocean bottom water characteristics in CMIP5 models. *Geophysical Research Letters*, *40*(7), 1409–1414. https://doi.org/10.1002/grl.50287

Jenkins, A., Hellmer, H. H., & Holland, D. M. (2001). The role of meltwater advection in the formulation of conservative boundary conditions at an ice-ocean interface. *Journal of Physical Oceanography*, *31*(1), 285–296. https://doi.org/10.1175/1520-0485(2001)031<0285:tromai>2.0.co;2

Jongma, J. I., Driesschaert, E., Fichefet, T., Goosse, H., & Renssen, H. (2009). The effect of dynamic–thermodynamic icebergs on the Southern Ocean climate in a three-dimensional model. *Ocean Modelling*, *26*(1–2), 104–113. https://doi.org/10.1016/j.ocemod.2008.09.007

Joughin, I., & MacAyeal, D. R. (2005). Calving of large tabular icebergs from ice shelf rift systems. *Geophysical Research Letters*, *32*(2), L02501. https://doi.org/10.1029/2004GL020978

Jullion, L., Naveira Garabato, A. C., Meredith, M. P., Holland, P. R., Courtois, P., & King, B. A. (2013). Decadal freshening of the Antarctic Bottom Water exported from the Weddell Sea. *Journal of Climate*, *26*(20), 8111–8125. https://doi.org/10.1175/JCLI-D-12-00765.1

Killworth, P. D. (1983). Deep convection in the world ocean. *Reviews of Geophysics*, *21*(1), 1–26. https://doi.org/10.1029/RG021i001p00001

Lee, S.-K., Lumpkin, R., Baringer, M. O., Meinen, C. S., Goes, M., Dong, S., et al. (2019). Global meridional overturning circulation inferred from a data-constrained ocean & sea-ice model. *Geophysical Research Letters*, *45*(3), 1521–1530. https://doi.org/10.1029/2018GL080940

Lee, S.-K., Volkov, D., Lopez, H., Cheon, W. G., Gordon, A. L., Liu, Y., & Wanninkhof, R. (2017). Wind-driven ocean dynamics impact on the contrasting sea-ice trends around West Antarctica. *Journal of Geophysical Research: Oceans*, *122*(5), 4413–4430. https://doi.org/10.1002/2016JC012416

Menezes, V. V., Macdonald, A. M., & Schatzman, C. (2017). Accelerated freshening of Antarctic Bottom Water over the last decade in the Southern Indian Ocean. *Science Advances*, *3*(1). https://doi.org/10.1126/sciadv.1601426

Mensah, V., Nakayama, Y., Fujii, M., Nogi, Y., & Ohshima, K. I. (2021). Dense water downslope flow and AABW production in a numerical model: Sensitivity to horizontal and vertical resolution in the region off cape Darnley polynya. *Ocean Modelling*, *165*, 101843. https://doi.org/10.1016/j.ocemod.2021.101843

Nowicki, S., & Seroussi, H. (2018). Projections of future sea-level contributions from the Greenland and Antarctic ice sheets: Challenges beyond dynamical ice sheet modelling. *Oceanography*, *31*(2). https://doi.org/10.5670/oceanog.2018.216

Orsi, A. H., Johnson, G. C., & Bullister, J. L. (1999). Circulation, mixing, and production of Antarctic Bottom Water. *Progress in Oceanography*, *43*(1), 55–109. https://doi.org/10.1016/S0079-6611(99)00004-X

Parkinson, C. L., & Cavalieri, D. J. (2012). Antarctic sea ice variability and trends, 1979–2010. *The Cryosphere*, *6*(4), 871–880. https://doi.org/10.5194/tc-6-871-2012

Pauling, A. G., Bitz, C. M., Smith, I. J., & Langhorne, P. J. (2016). The response of the Southern Ocean and Antarctic sea ice to fresh water from ice shelves in an Earth System Model. *Journal of Climate*, *29*(5), 1655–1672. https://doi.org/10.1175/jcli-d-15-0501.1

Purkey, S. G., & Johnson, G. C. (2012). Global contraction of Antarctic Bottom Water between the 1980s and 2000s. *Journal of Climate*, *25*(17), 5830–5844. https://doi.org/10.1175/JCLI-D-11-00612.1

Purkey, S. G., Johnson, G. C., Talley, L. D., Sloyan, B. M., Wijffels, S. E., Smethie, W., et al. (2019). Unabated bottom water warming and freshening in the South Pacific Ocean. *Journal of Geophysical Research: Oceans*, *124*(3), 1778–1794. https://doi.org/10.1029/2018JC014775

Rignot, E., Jacobs, S., Mouginot, J., & Scheuchl, B. (2013). Ice-shelf melting around Antarctica. *Science*, *341*(6143), 266–270. https://doi.org/10.1126/science.1235798

Rignot, E., Mouginot, J., Scheuchl, B., Van Den Broeke, M., Van Wessem, M. J., & Morlighem, M. (2019). Four decades of Antarctic Ice Sheet mass balance from 1979–2017. *Proceedings of the National Academy of Sciences*, *116*(4), 1095–1103. https://doi.org/10.1073/pnas.1812883116

Shimada, K., Aoki, S., Ohshima, K. I., & Rintoul, S. R. (2012). Influence of Ross Sea Bottom Water changes on the warming and freshening of the Antarctic Bottom Water in the Australian-Antarctic Basin. *Ocean Science*, *8*(4), 419–432. https://doi.org/10.5194/os-8-419-2012

Silvano, A., Rintoul, S. R., Peña-Molino, B., Hobbs, W. R., van Wijk, E., Aoki, S., et al. (2018). Freshening by glacial meltwater enhances melting of ice shelves and reduces formation of Antarctic Bottom Water. *Science Advances*, *4*(4). https://doi.org/10.1126/sciadv.aap9467

Solodoch, A., Stewart, A. L., Hogg, A. M., Morrison, A. K., Kiss, A. E., Thompson, A. F., et al. (2022). How does Antarctic Bottom Water cross the Southern Ocean? *Geophysical Research Letters*, *49*(7). https://doi.org/10.1029/2021GL097211

Steele, M., Morley, R., & Ermold, W. (2001). PHC: A global ocean hydrography with a high-quality Arctic Ocean. *Journal of Climate*, *14*(9), 2079–2087. https://doi.org/10.1175/1520-0442(2001)014<2079:PAGOHW>2.0.CO;2

Sun, S., & Eisenman, I. (2021). Observed Antarctic sea ice expansion reproduced in a climate model after correcting biases in sea ice drift velocity. *Nature Communications*, *12*(1), 1060. https://doi.org/10.1038/s41467-021-21412-z

Talley, L. D. (2013). Closure of the global overturning circulation through the Indian, Pacific, and Southern Oceans: Schematics and transports. *Oceanography*, *26*(1), 80–97. https://doi.org/10.5670/oceanog.2013.07

Tsujino, H., Urakawa, L. S., Griffies, S. M., Danabasoglu, G., Adcroft, A. J., Amaral, A. E., et al. (2020). Evaluation of global ocean–sea-ice model simulations based on the experimental protocols of the Ocean Model Intercomparison Project phase 2 (OMIP-2). *Geoscientific Model Development*, *13*(8), 3643–3708. https://doi.org/10.5194/gmd-13-3643-2020

Wagner, T. J. W., Dell, R., & Eisenman, I. (2017). An analytical model of iceberg drift. *Journal of Physical Oceanography*, *47*(7), 1605–1616. https://doi.org/10.1175/jpo-d-16-0262.1

Wijk, E. M., & Rintoul, S. R. (2014). Freshening drives contraction of Antarctic Bottom Water in the Australian Antarctic Basin. *Geophysical Research Letters*, *41*(5), 1657–1664. https://doi.org/10.1002/2013GL058921

References From the Supporting Information

Abrahamsen, E. P., Meijers, A. J. S., Polzin, K. L., Naveira Garabato, A. C., King, B. A., Firing, Y. L., et al. (2019). Stabilization of dense Antarctic water supply to the Atlantic Ocean overturning circulation. *Nature Climate Change*, *9*(10), 742–746. https://doi.org/10.1038/s41558-019-0561-2

Barbat, M. M., Rackow, T., Hellmer, H. H., Wesche, C., & Mata, M. M. (2019). Three years of near-coastal Antarctic iceberg distribution from a machine learning approach applied to SAR imagery. *Journal of Geophysical Research: Oceans*, *124*(9), 6658–6672. https://doi.org/10.1029/2019jc015205

Bishop, S. P., Gent, P. R., Bryan, F. O., Thompson, A. F., Long, M. C., & Abernathey, R. (2016). Southern Ocean overturning compensation in an eddy-resolving climate simulation. *Journal of Physical Oceanography*, *46*(5), 1575–1592. https://doi.org/10.1175/jpo-d-15-0177.1

Briegleb, B. P., Danabasoglu, G., & Large, W. G. (2010). An overflow parameterization for the ocean component of the Community Climate System Model. National Center for Atmospheric Research Technical Note NCAR/TN-4811STR. https://doi.org/10.5065/D69K4863

Broecker, W. (2010). *The great ocean conveyor.* Princeton University Press.

Chassignet, E. P., Yeager, S. G., Fox-Kemper, B., Bozec, A., Castruccio, F., Danabasoglu, G., et al. (2020). Impact of horizontal resolution on global ocean–sea ice model simulations based on the experimental protocols of the Ocean Model Intercomparison Project phase 2 (OMIP-2). *Geoscientific Model Development*, *13*(9), 4595–4637. https://doi.org/10.5194/gmd-13-4595-2020

Cheon, W. G., Lee, S. K., Gordon, A. L., Liu, Y., Cho, C. B., & Park, J. J. (2015). Replicating the 1970s' Weddell polynya using a coupled ocean-sea ice model with reanalysis surface flux fields. *Geophysical Research Letters*, *42*(13), 5411–5418. https://doi.org/10.1002/2015GL064364

Dias, F. B., Domingues, C. M., Marsland, S. J., Rintoul, S. R., Uotila, P., Fiedler, R., et al. (2021). Subpolar Southern Ocean response to changes in the surface momentum, heat, and freshwater fluxes under 2xCO2. *Journal of Climate*, *34*(21), 8755–8775. https://doi.org/10.1175/jcli-d-21-0161.1

Dotto, T. S., Kerr, R., Mata, M. M., Azaneu, M., Wainer, I. E. K. C., Fahrbach, E., & Rohardt, G. (2014). Assessment of the structure and variability of Weddell Sea water masses in distinct ocean reanalysis products. *Ocean Science*, *10*(3), 523–546. https://doi.org/10.5194/os-10-523-2014

Foldvik, A., Gammelsrød, T., & Tørresen, T. (1985). Circulation and water masses on the southern Weddell Sea shelf. *Oceanology of the Antarctic continental shelf*, *43*, 5–20. https://doi.org/10.1029/AR043p0005

Gordon, A. L. (1986). Is there a global scale ocean circulation? *Eos, Transactions American Geophysical Union*, *67*(9), 109–110. https://doi.org/10.1029/EO067i009p00109

Hewitt, H. T., Roberts, M., Mathiot, P., Biastoch, A., Blockley, E., Chassignet, E. P., et al. (2020). Resolving and parameterising the ocean mesoscale in Earth system models. *Current Climate Change Reports*, *6*(4), 137–152. https://doi.org/10.1007/s40641-020-00164-w

Jeong, H., Asay-Davis, X. S., Turner, A. K., Comeau, D. S., Price, S. F., Abernathey, R. P., et al. (2020). Impacts of ice-shelf melting on water-mass transformation in the Southern Ocean from E3SM simulations. *Journal of Climate*, *33*(13), 5787–5807. https://doi.org/10.1175/JCLI-D-19-0683.1

Johnson, G. C. (2008). Quantifying Antarctic Bottom Water and North Atlantic deep water volumes. *Journal of Geophysical Research*, *113*(C5), C05027. https://doi.org/10.1029/2007JC004477

Kerr, R., Dotto, T. S., Mata, M. M., & Hellmer, H. H. (2018). Three decades of deep water mass investigation in the Weddell Sea (1984–2014): Temporal variability and changes. *Deep Sea Research Part II: Topical Studies in Oceanography*, *149*, 70–83. https://doi.org/10.1016/j.dsr2.2017.12.002

Large, W., & Yeager, S. G. (2009). The global climatology of an interannually varying air–sea flux data set. *Climate Dynamics*, *33*(2), 341–364. https://doi.org/10.1007/s00382-008-0441-3

Mackie, S., Smith, I. J., Ridley, J. K., Stevens, D. P., & Langhorne, P. J. (2020). Climate response to increasing Antarctic iceberg and ice shelf melt. *Journal of Climate*, *33*(20), 8917–8938. https://doi.org/10.1175/JCLI-D-19-0881.1

Merino, N., Le Sommer, J., Durand, G., Jourdain, N. C., Madec, G., Mathiot, P., & Tournadre, J. (2016). Antarctic icebergs melt over the Southern Ocean: Climatology and impact on sea ice. *Ocean Modelling*, *104*, 99–110. https://doi.org/10.1016/j.ocemod.2016.05.001

Nicholls, K. W., Østerhus, S., Makinson, K., Gammelsrød, T., & Fahrbach, E. (2009). Ice-ocean processes over the continental shelf of the southern Weddell Sea, Antarctica: A review. *Reviews of Geophysics*, *47*(3). https://doi.org/10.1029/2007RG000250

Nihashi, S., & Ohshima, K. I. (2015). Circumpolar mapping of Antarctic coastal polynyas and landfast sea ice: Relationship and variability. *Journal of Climate*, *28*(9), 3650–3670. https://doi.org/10.1175/JCLI-D-14-00369.1

Orsi, A. H., & Wiederwohl, C. L. (2009). A recount of Ross Sea waters. *Deep Sea Research Part II: Topical Studies in Oceanography*, *56*(13–14), 778–795. https://doi.org/10.1016/j.dsr2.2008.10.033

Purich, A., & England, M. H. (2021). Historical and future projected warming of Antarctic Shelf Bottom Water in CMIP6 models. *Geophysical Research Letters*, *48*(10), e2021GL092752. https://doi.org/10.1029/2021GL092752

Ribeiro, N. (2020). Exploring the Antarctic waters with seals in electric hats. *Nature Reviews Earth & Environment*, *1*(6), 282. https://doi.org/10.1038/s43017-020-0056-8

Shu, Q., Wang, Q., Song, Z., Qiao, F., Zhao, J., Chu, M., & Li, X. (2020). Assessment of sea ice extent in CMIP6 with comparison to observations and CMIP5. *Geophysical Research Letters*, *47*(9), e2020GL087965. https://doi.org/10.1029/2020GL087965

Silvano, A., Foppert, A., Rintoul, S. R., Holland, P. R., Tamura, T., Kimura, N., et al. (2020). Recent recovery of Antarctic Bottom Water formation in the Ross Sea driven by climate anomalies. *Nature Geoscience*, *13*(12), 780–786. https://doi.org/10.1038/s41561-020-00655-3

Singh, H. K., Landrum, L., Holland, M. M., Bailey, D. A., & DuVivier, A. K. (2021). An overview of Antarctic sea ice in the Community Earth System Model version 2, Part I: Analysis of the seasonal cycle in the context of sea ice thermodynamics and coupled atmosphere-ocean-ice processes. *Journal of Advances in Modeling Earth Systems*, *13*(3), e2020MS002143. https://doi.org/10.1029/2020MS002143

Stouffer, R. J., Seidov, D., & Haupt, B. J. (2007). Climate response to external sources of freshwater: North Atlantic vs. the Southern Ocean. *Journal of Climate*, *20*(3), 436–448. https://doi.org/10.1175/jcli4015.1

Whitworth, T., & Orsi, A. H. (2006). Antarctic Bottom Water production and export by tides in the Ross Sea. *Geophysical Research Letters*, *33*(12), L12609. https://doi.org/10.1029/2006GL026357

Williams, G. D., Bindoff, N. L., Marsland, S. J., & Rintoul, S. R. (2008). Formation and export of dense shelf water from the Adélie Depression, East Antarctica. *Journal of Geophysical Research*, *113*(C4), C04039. https://doi.org/10.1029/2007JC004346

Williams, G. D., Herraiz-Borreguero, L., Roquet, F., Tamura, T., Ohshima, K. I., Fukamachi, Y., et al. (2016). The suppression of Antarctic Bottom Water formation by melting ice shelves in Prydz Bay. *Nature Communications*, *7*(1), 1–9. https://doi.org/10.1038/ncomms12577